Supplementary Information:

Synaptotagmin-1 C2B domains cooperatively stabilize the fusion stalk via a master-servant mechanism

Ary Lautaro Di Bartolo[†,‡] and Diego Masone[*,†,¶]

†*Instituto de Histología y Embriología de Mendoza (IHEM) - Consejo Nacional de Investigaciones Científicas y Técnicas (CONICET), Universidad Nacional de Cuyo (UNCuyo), 5500, Mendoza, Argentina*

‡*Facultad de Ciencias Exactas y Naturales, Universidad Nacional de Cuyo (UNCuyo), 5500, Mendoza, Argentina*

¶*Facultad de Ingeniería, Universidad Nacional de Cuyo (UNCuyo), 5500, Mendoza, Argentina*

E-mail: diego.masone@ingenieria.uncuyo.edu.ar

Umbrella sampling technical details

We performed umbrella sampling using PLUMED. For each window, depending on its individual drift, additional simulation time was added for totals varying between 110ns and 210ns. Transient regimes were individually discarded to get in all cases at least 100ns in the steady-state regime.

For membranes-only system equilibrium points (ξ_{f0}) for each window were distributed as follows: 0.20, 0.25, 0.30, 0.35, 0.40, 0.45, 0.50, 0.55, 0.56, 0.57, 0.58, 0.60, 0.65, 0.70, 0.75,

0.80 and 0.85. In all cases a force constant of k=30,000 kJ/mol was used. Figure S1a shows convergence of the energy profile in the membranes-only system. As observed, there are no significant differences between 90ns and 100ns. Besides, figure S1b shows histograms of the order parameters for all 17 windows.

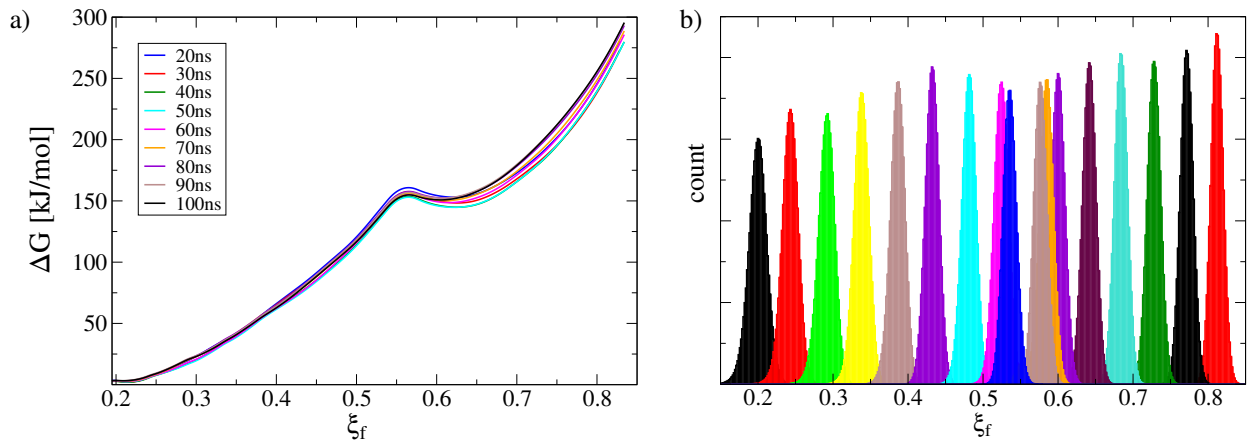

Figure S1: **Umbrella sampling convergence analysis for membranes-only system. a)** Free energy profiles at different simulation times in the steady-state regime. **b)** Histogram superposition for umbrella sampling simulations. A set of 17 windows was used to recover free energy profiles.

For simulation system including one Syt1-C2B wild-type domain, equilibrium points (ξ_{f0}) for each window were distributed as follows: 0.20, 0.25, 0.30, 0.35, 0.40, 0.45, 0.50, 0.52, 0.55, 0.56, 0.565, 0.58, 0.60, 0.65, 0.70, 0.75, 0.80 and 0.85. In all cases a force constant of k=30,000 kJ/mol was used. Figure S2a shows convergence of the energy profile in the system containing one Syt1-C2B wild-type domain. As observed, there are no significant differences between 90ns and 100ns. Besides, figure S2b shows histograms of the order parameters for all 18 windows.

For simulation system including two Syt1-C2B wild-type domains, equilibrium points (ξ_{f0}) for each window were distributed as follows: 0.20, 0.25, 0.30, 0.35, 0.40, 0.45, 0.50, 0.55, 0.58, 0.60, 0.625, 0.65, 0.70, 0.75, 0.80 and 0.85. In all cases a force constant of k=30,000 kJ/mol was used. Figure S3a shows convergence of the energy profile in the system containing two Syt1-C2B wild-type domains. Progressive zoom insets detail free energy differences. As observed, there are no significant differences between 90ns and 100ns. Besides, figure S3b

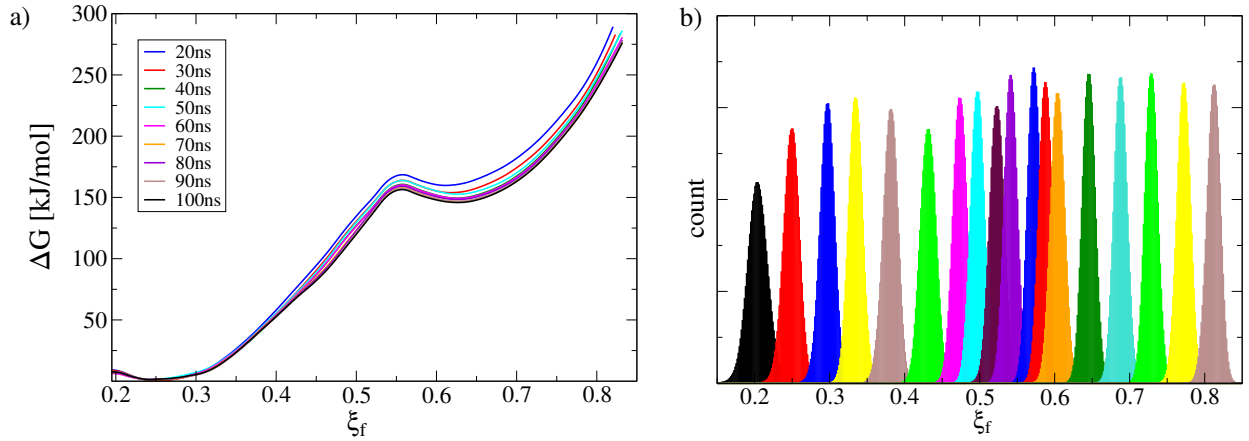

Figure S2: **Umbrella sampling convergence analysis for simulation system including 1 Syt1-C2B wild-type domain. a)** Free energy profiles at different simulation times in the steady-state regime. **b)** Histogram superposition for umbrella sampling simulations. A set of 18 windows was used to recover free energy profiles.

shows histograms of the order parameters for all 16 windows.

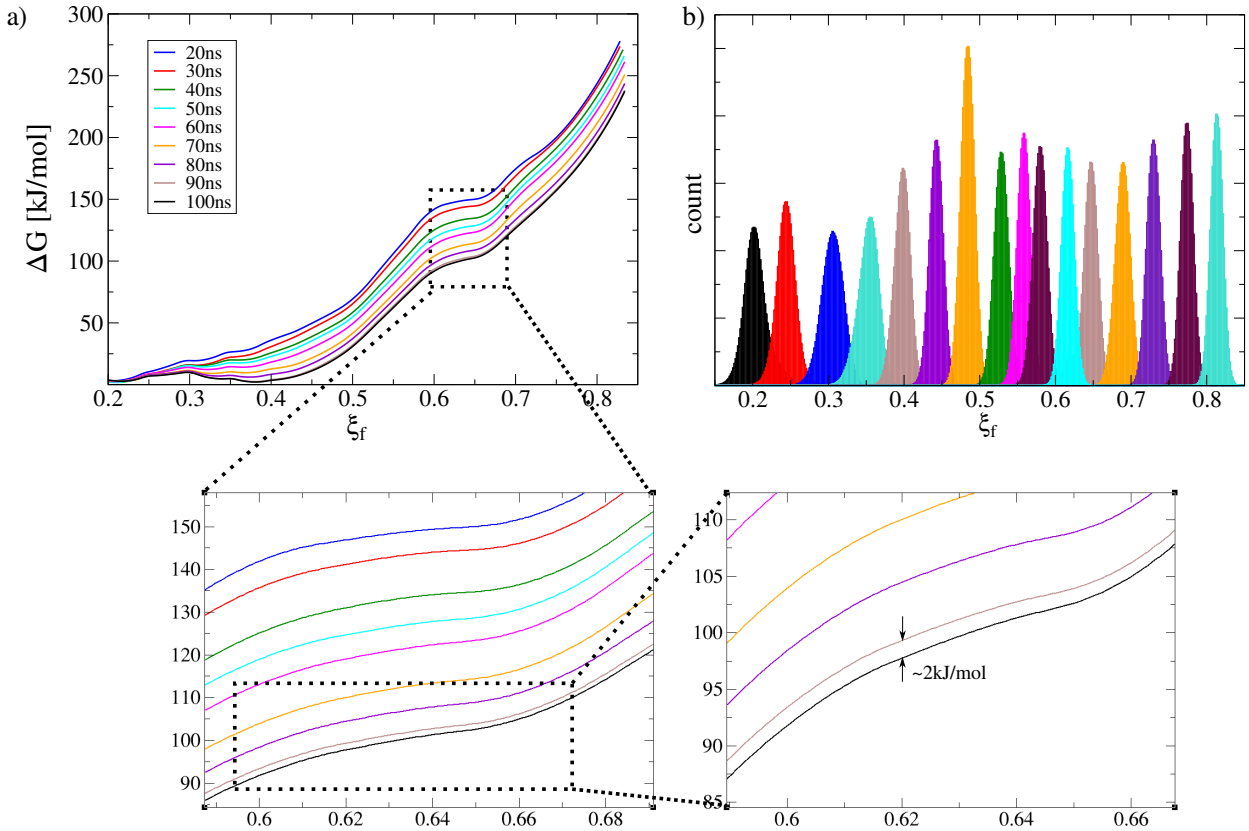

Figure S3: **Umbrella sampling convergence analysis for simulation system including two Syt1-C2B wild-type domains. a)** Free energy profiles at different simulation times in the steady-state regime. Progressive zooms show the difference in free energy between last two PMFs (90ns and 100ns). **b)** Histogram superposition for umbrella sampling simulations. A set of 16 windows was used to recover free energy profiles.

For simulation system including two Syt1-C2B mutant T328E-T329 domains, equilibrium points (ξ_{f0}) for each window were distributed as follows: 0.20, 0.25, 0.30, 0.35, 0.40, 0.45, 0.50, 0.55, 0.58, 0.60, 0.65, 0.70, 0.725, 0.75, 0.80 and 0.85. In all cases a force constant of k=30,000 kJ/mol was used. Figure S4a shows convergence of the energy profile in the system containing two Syt1-C2B mutant T328E-T329 domains. As observed, there are no significant differences between 90ns and 100ns. Besides, figure S4b shows histograms of the order parameters for all 16 windows.

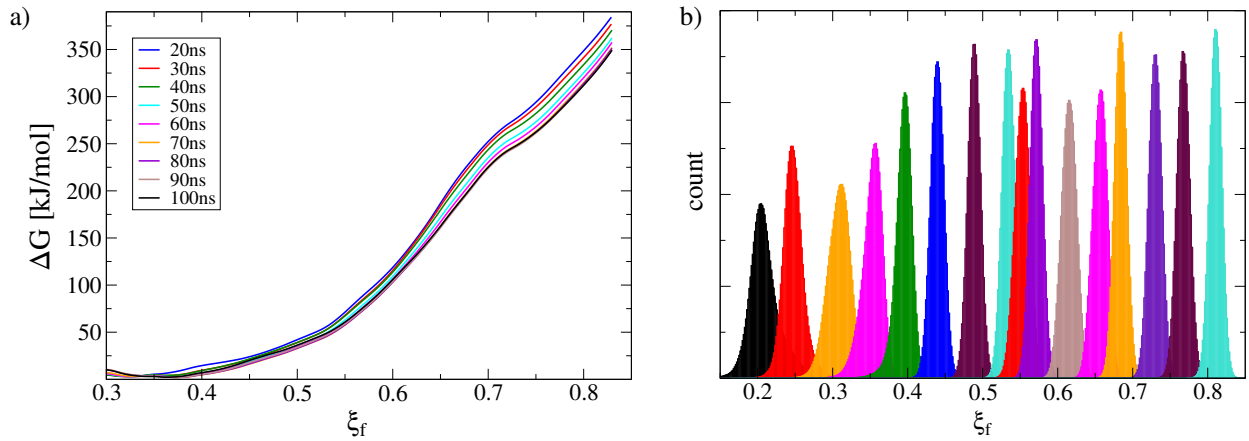

Figure S4: **Umbrella sampling convergence analysis for simulation system including two Syt1-C2B mutant T328E-T329E domains. a)** Free energy profiles at different simulation times in the steady-state regime. **b)** Histogram superposition for umbrella sampling simulations. A set of 16 windows was used to recover free energy profiles.

Figure S5 shows time-averaged densities during stalk formation for selected values of the collective variable. The three species of lipids used along this work are distinctly colored.

Unbiased molecular dynamics: from initially flat and parallel bilayers

We performed 5μs of unbiased molecular dynamics starting from initially flat and parallel bilayers, for the three main cases studied in this work: membranes-only, with 2 Syt1-C2B wild-type domains and with 2 Syt1-C2B mutant domains. Figure S6 shows molecular dynamics snapshots at t=1μs, wild-type domains are blue and mutant ones are green.

Figure S7 shows lipid density profiles for the systems containing 2 C2B domains (wild-type and mutant). From all three panels, PIP_2 and POPS lipids show the most significant

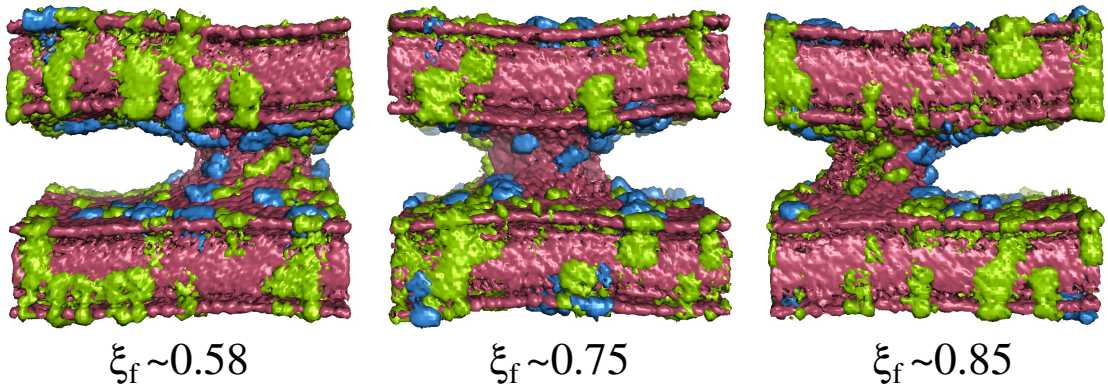

Figure S5: **Time averaged densities during stalk evolution**. Colors are assigned as follows: POPC in red, POPS in green and PIP_2 in blue. Water molecules are not shown.

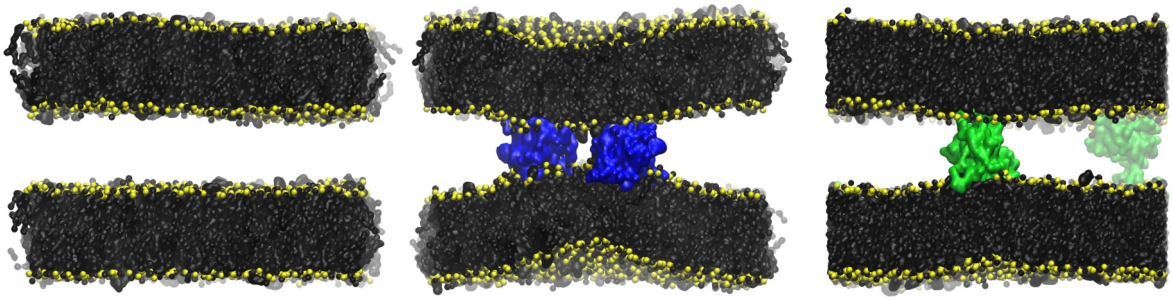

Figure S6: **Molecular dynamics snapshots at t=1μs.** Lipid molecules are shown in black with PO4 beads in yellow. Wild-type Syt1-C2B domains are blue and mutant ones are green.

difference between wild-type and mutant systems. This observation supports the evidence that wild-type C2B domains pull from PIP_2 lipids to bring membranes together, in agreement with Radial Distribution Functions (RDF) in figure 6 in the main text.

Alternatively, figure S8 shows RDFs for POPS. Panel S8a shows measurements for R398 and R399 for 2 Syt1-C2B wild-type and 2 Syt1-C2B mutant domains. Analogously, panel S8b shows measurements for K326 and K327 in the same C2B domains. It can be observed that residues R398,R399 and K326,K327 show significant differences in their affinity to POPS in both master and servant mutant domains (red and green lines) when respectively compared to their wild-type counterparts. We hypothesize that the reduced binding to PIP2 of E328,E329 in the mutated polybasic region of C2B domains (both master and servant), allows for other key residues (such as, K326,K327 and R398,R399) to intensify their interactions with other

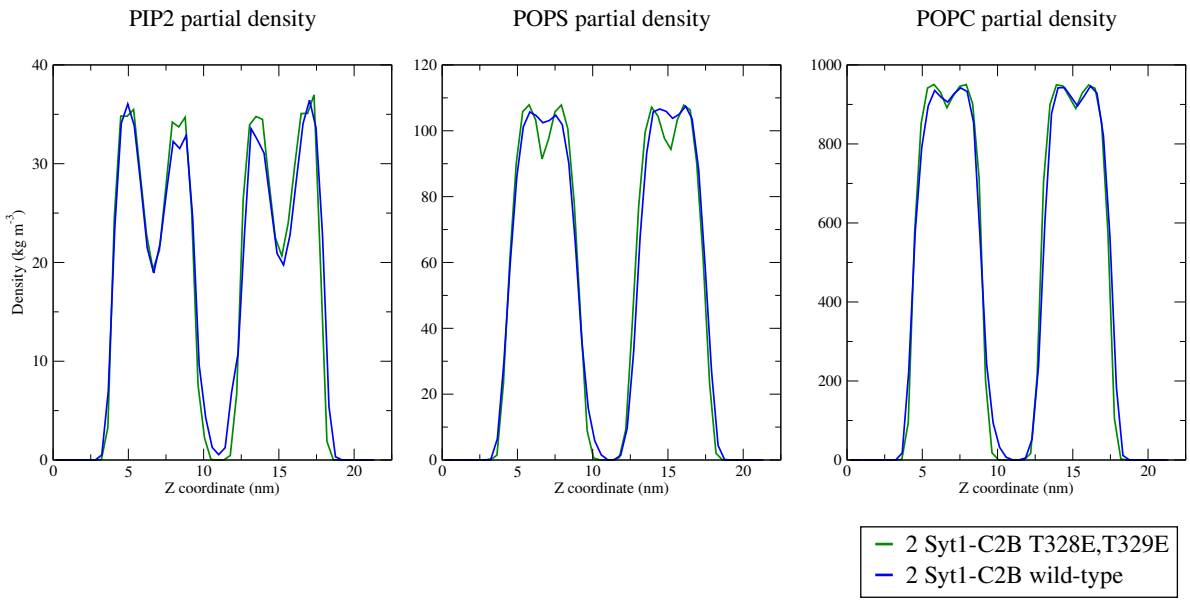

Figure S7: **Lipid species density profiles.** Profiles show systems with 2 Syt1-C2B wild-type domains (blue) and with 2 Syt1-C2B mutant domains (green).

acidic membrane lipids (such as POPS), hence altering the POPS density profiles in figure S7.

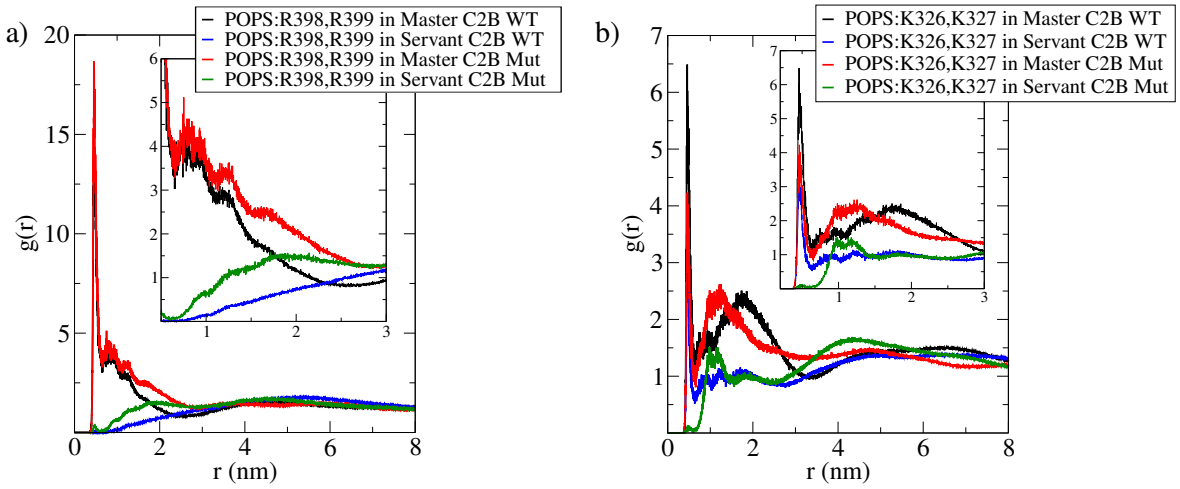

Figure S8: **Radial distribution functions with POPS lipids. a)** For R398 and R399 in C2B domains. **b)** For K326 and K327 in C2B domains.

Figure S9 shows the minimum PO4:PO4 distance along Z axis as a function of the radial XY distance to the center of the defect (where most probably the stalk will form). It can be observed that 2 Syt1-C2B wild-type domains (blue line) locally pulls membrane together

to a minimum inter-membrane distance of ∼1.5nm. On the contrary, both membranes-only and mutant domains systems keep the inter-membrane separation above 3nm, as already suggested by molecular dynamics snapshots in figure S6.

Figure S9 also verifies that the defect is initially a local deformation, meaning that all curves converge to ∼4.25nm for radial distances far enough from the defect (∼6.5nm).

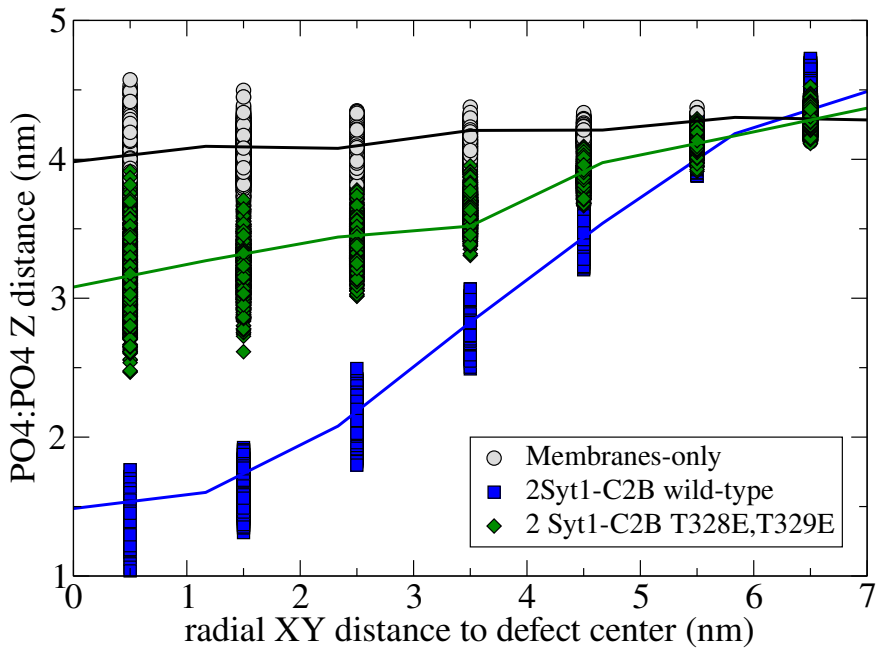

Figure S9: **PO4:PO4 Z distance as a function of the radial XY distance to the center of the defect.** Data shows membranes-only system (black line), with 2 Syt1-C2B wild-type domains (blue) and with 2 Syt1-C2B mutant domains (green).

Figure S10 shows the orientation of each C2B domain along unbiased molecular dynamics for wild-type domains (S10a) and mutant ones (S10b). Analogously to figure 5a in the main text, (besides the non-linear relation in eq. 1) each domain orientation is now measured with angle α, as defined geometrically in panel S10c and by the following equation:

$$\alpha = atan\frac{D_z}{D_{xy}} \tag{1}$$

Therefore, higher values of α correspond to higher values of the end-to-end distance projected along Z axis (D_z). As observed before in figure 5a in the main text, the master protein shows systematically higher values of D_z (and of α) than its servant, either for wild-type or mutant forms.

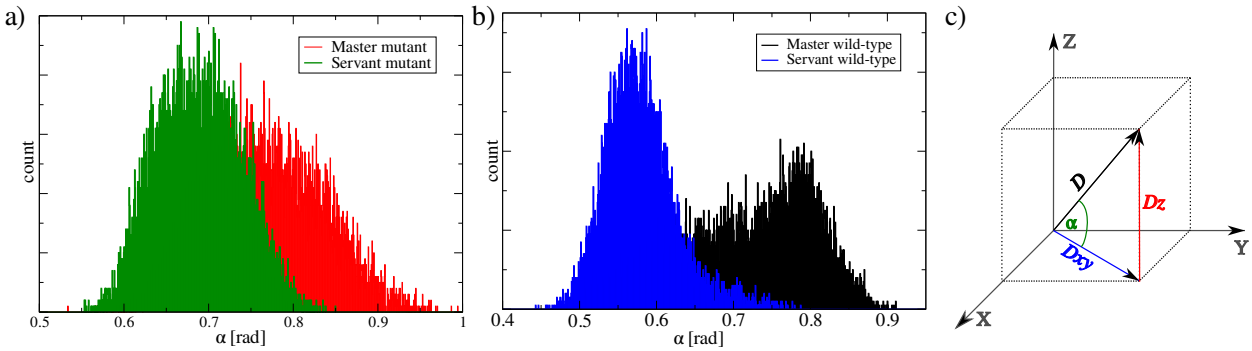

Figure S10: **C2B domains orientation.** **a)** Two wild-type domains. **b)** Two mutant domains. **c)** Schematics to define angle α and its relation with the end-to-end Z distance (D_z).

Unbiased molecular dynamics: from a $\xi_f \sim 0.85$ fusion stalk

We performed 10μs of unbiased molecular dynamics starting from a fusion stalk initially set at $\xi_f \sim 0.85$. Figure S11a shows the inter-membrane amount of lipids. Both curves describe how the fusion stalk stabilizes at ∼175 lipids. This amount of lipids is in agreement with figure 2b in the main text. Also, when the stalk is released from its restraint ($\xi_f \sim 0.85$ at t=0μs in figure S11) under both situations (with 2 wild-type and 2 mutant domains) the amount of lipids in the inter-membrane space increases. Initial values in this figure are in agreement with the amount of lipids measured under the collective variable restraint in figure 4a in the main text.

For long simulation times in unbiased conditions, the stalk tends to stretch when C2B domains are present. Figure S12 shows the shape of the stalk after several μs of unbiased simulation for membranes-only (panel S12a) and in the presence of 2 C2B domains (S12b for wild-types and S12c for mutants T328E,T329E). The elongated shapes of the stalk on panels S12b and S12c correspond to the stabilization points at $\xi_f \sim 0.6$ in figure S11b.

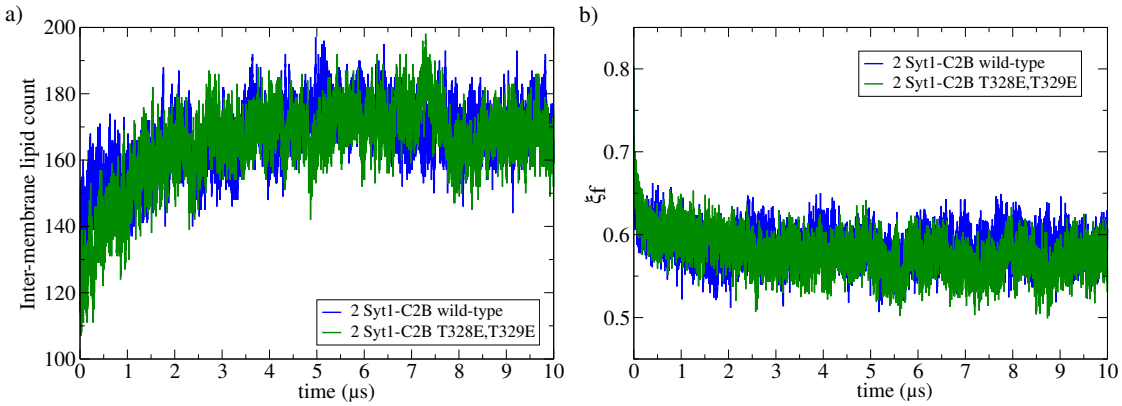

Figure S11: **Unbiased molecular dynamics initiated from a fusion stalk. a)** Inter-membrane lipid count and **b)** ξ_f evolution over time. Measured for systems containing 2 wild-type Syt1-C2B (blue lines) and 2 mutant Syt1-C2B domains (green lines).

ξ_f collective variable

Eq. 1 in the main text, defines collective variable ξ_f as originally developed by Prof. Hub and collaborators. ξ_f uses a membrane spanning cylinder that is decomposed into slices along the Z axis normal to the bilayers. The cylinder is defined by the number of cylinder slices (N_{sf}), their thickness (d_{sf}), their radius (R_{cylf}) and their occupation factor (ζ_{sf}), see eqs. 2 and 3. See figure S13.

Then, ξ_f counts the fraction of slices that are occupied by a group of beads (in this work: C4A,C4B and C5A tail beads, see figure S14). This definition of the collective variable makes lipids to approximate and tilt while membranes fuse. The result is a well-defined fusion stalk. Explicitly, ${N_{sf}}^{(p)}$ accounts for the number of beads within slice s inside the membrane-spanning cylinder. δ_{sf} is a continuous function ranging from 0 (for no beads in slice s) to 1 (for 1 or more beads in slice s) as defined in eq. 2.

$$\delta_{sf}({N_{sf}}^{(p)}) = \psi({N_{sf}}^{(p)}; \zeta_f) \tag{2}$$

Switching piecewise-defined function for ξ_f is linear-exponential, continuous and differentiable, as shown in eq. 3.

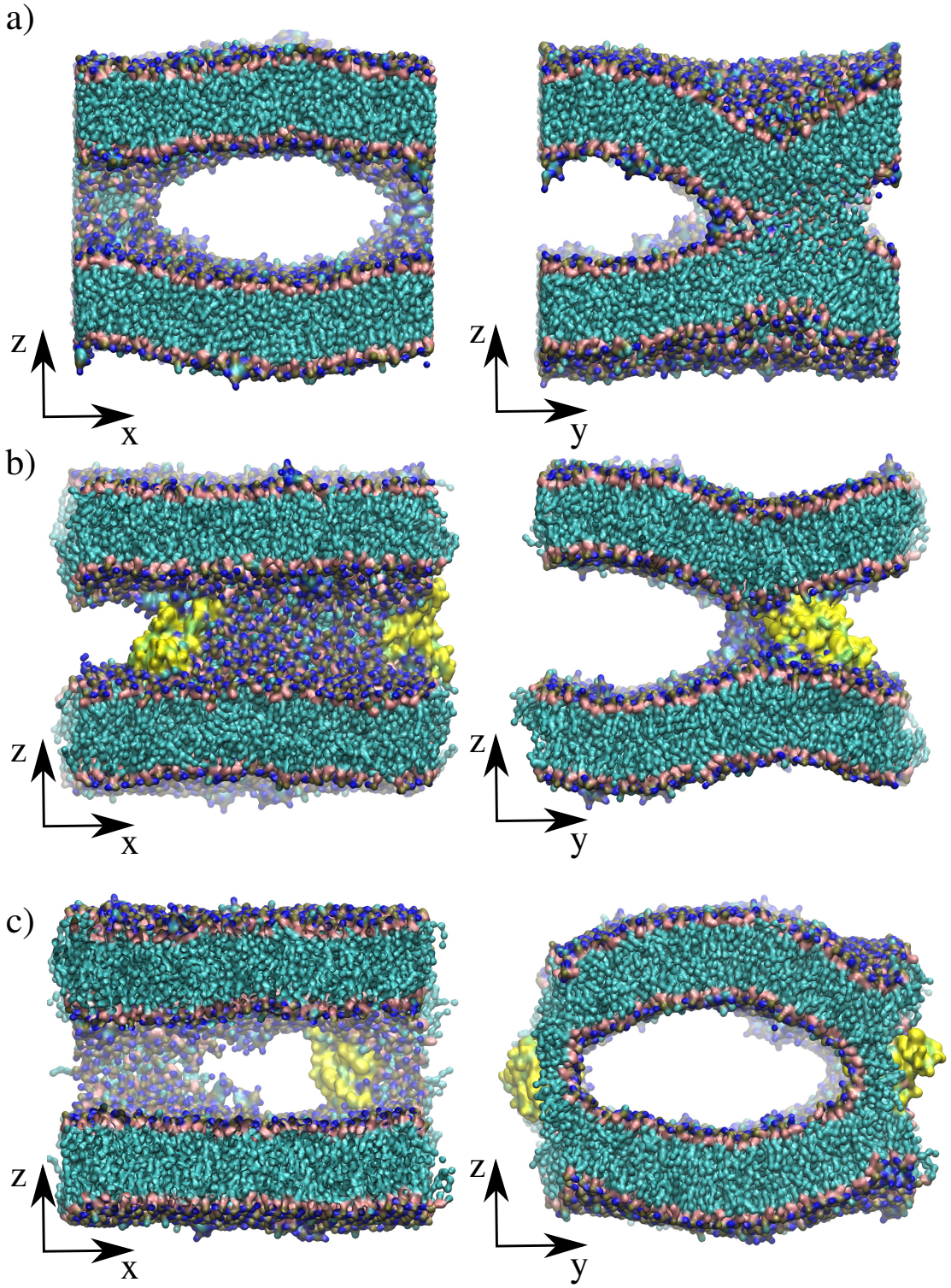

Figure S12: **Stalk shape elongation during 10μs of unbiased molecular dynamics. a)** Membranes-only system. **b)** With two wild-type C2B domains. **c)** With two T328E,T329E C2B domains. For simulation times in the μs scale, C2B interactions with the lipid bilayers make the stalk to elongate.

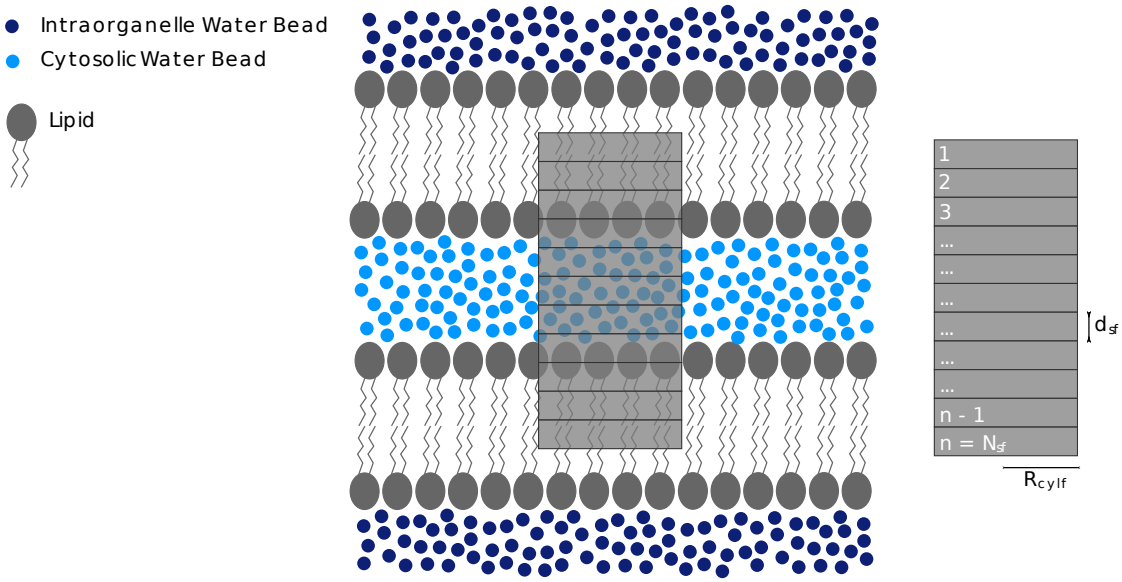

Figure S13: **Schematics of the membrane spanning cylinder to induce fusion used by collective variable ξ_f.** References on the right indicate the variables that define the shape of cylinder.

$$\psi(x;\zeta_f) = \begin{cases} \zeta_f x & if \quad x \leq 1 \\ \\ 1 - ce^{-bx} & if \quad x > 1 \end{cases} \tag{3}$$

Parameters, b and c are defined as a function of the occupation factor ζ_f (see eqs. 4 and 5).

$$b = \frac{\zeta_f}{1 - \zeta_f} \tag{4}$$

$$c = (1 - \zeta_f)e^b \tag{5}$$

As we have done before in previous studies and to acknowledge Prof. Hub's work, we kept the same nomenclature as the original publication. We have only added the sub-index f to each variable to highlight that it is being used for membrane fusion.

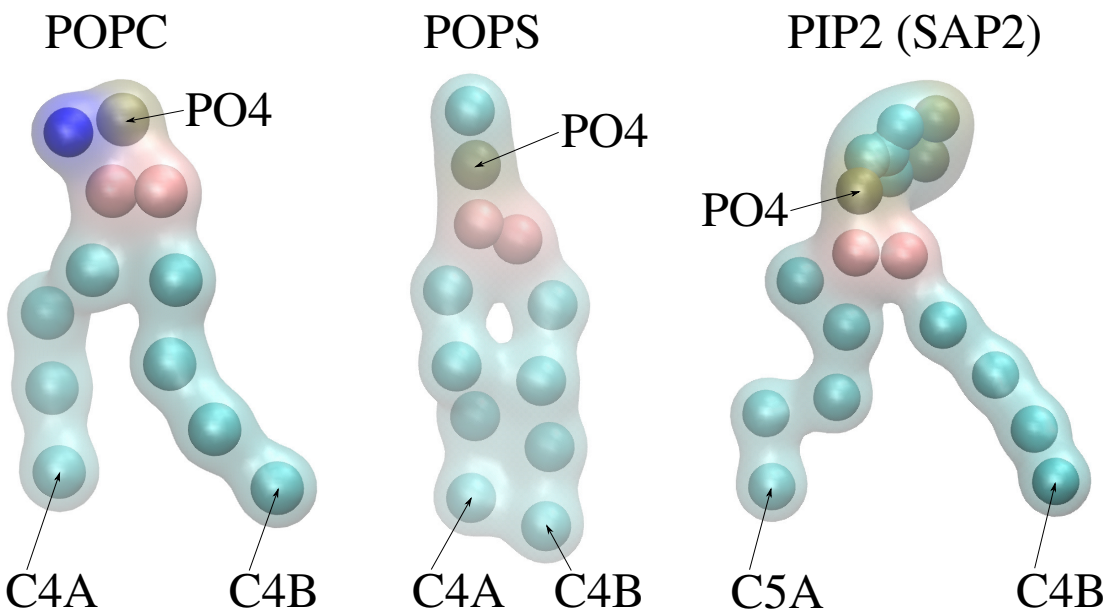

Figure S14: **MARTINI POPC, POPS and PIP2 lipids**. Bead labels are standard names for MARTINI.

Radial Distribution Function calculations

Radial distribution functions (RDF) were calculated with GROMACS built-in *gmx rdf* function. Conceptually, a normalized RDF is the probability of finding a group of particles at a distance r from another group of particles. We have used radial distribution functions $g(r)$ to quantify C2B domains statistical coordination (and their specific regions of interest) with the three species of lipids in the bilayers (POPC, POPS and PIP2), as function of the distance (r). As defined in GROMACS, $g_{AB}(r)$ is a pair correlation function between particles of types A and B, as follows:

$$g_{AB}(r) = \frac{< \rho_B(r) >}{< \rho_B >_{local}} \tag{6}$$

where $< \rho_B(r) >$ is the density of particles of type B at a distance r around particles of type A. Analogously, $< \rho_B >_{local}$ is the density of particles of type B averaged over all spheres around particles A with radius equal to half of the simulation box $L_x/2$, for periodic boundary conditions (PBC). As defined in eq. 6, the radial distribution function is a ratio

of particle densities, making it a dimensionless quantity. The use of $g(r)$ as a measure of coordination between particles is direct: integrating $g(r)$ in spherical coordinates gives the coordination number of between groups of particles. For more details see GROMACS 2021 documentation: https://manual.gromacs.org/

Stalk formation in the presence of tandem C2A-C2B Syt1 domains

To analyze the effects on the free energy for stalk formation of a tandem C2A-C2B we have conducted PMF calculations using the crystal structure of the human synaptotagmin 1 C2A-C2B (PBD ID: 2R83). For adequate comparison, the rest of the system and the collective variable parameters were kept identical to the rest of the simulations along this work. Figure S15a shows the free energy profile for the C2A-C2B system (magenta line), compared to the rest of the systems. It can be observed that the total cost to reach the final state at $\xi_f \sim 0.85$ is slightly less than the wild-type C2B domains (blue line). Therefore, the tandem C2A-C2B also facilitates the formation of the fusion stalk, as extensively reported in the experimental literature. Remarkably, tandem C2A-C2B is known for bridging opposed bilayers and pulling them together. The rise in free energy in the interval $0.2 < \xi_f < 0.3$ reflects this effect, namely: equilibrium inter-membrane distance is strongly anchored by the presence of the tandem C2A-C2B domains at $\xi_f \sim 0.35$, making the free energy to rise as a response to any further attempt to reduce that value.

Additionally, we have conducted 5μs of unbiased simulations initiated from flat and parallel bilayers containing the C2A-C2B tandem in the inter-membrane space (the cytosol). Figure S15b shows the inter-membrane distance for this system together with the rest of the systems showed in figure 5b in the main text. It can be observed that tandem C2A-C2B domains significantly pull membranes together (to $\sim$1 nm), even below the system with 2 Syt1-C2B wild-type domains (see magenta and blue lines).

Although the inter-membrane distance is significantly reduced for the tandem C2A-C2B system, no further displacement to the right of the free energy zero reference is observed (red,

blue and green lines in figure S15a have the same free energy zero reference at $\xi_f \sim 0.35$, nevertheless with different inter-membrane distances S15b). This is due to a saturation effect intrinsic to the collective variable: once the spanning cylinder (see figure S13) is full (of tail beads) no further reduction of the inter-membrane distance has additional effects on the equilibrium value in the space of the collective variable.

Panels S15c and S15d show convergence analysis for the system with tandem C2A-C2B domains.

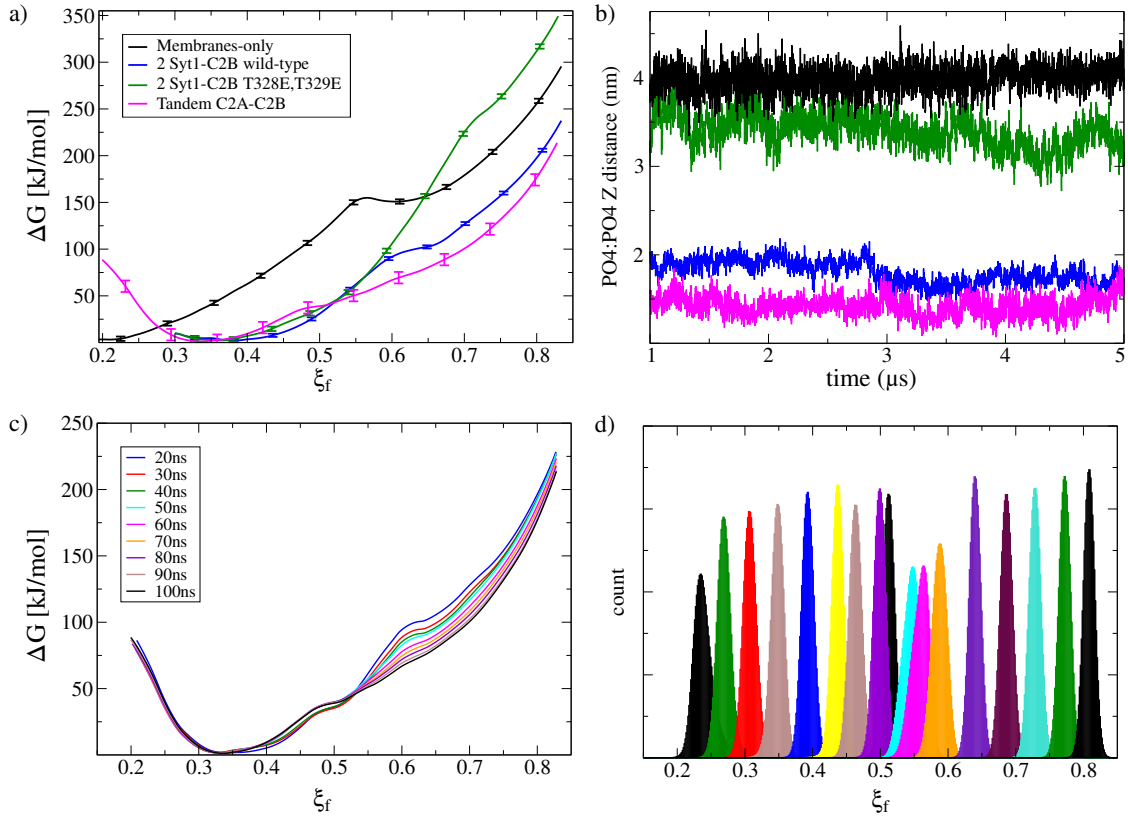

Figure S15: **Tandem C2A-C2B system**. **a)** PMF for fusion stalk formation. **b)** PO4:PO4 inter-membrane distance. **c)** Free energy profiles at different simulation times in the steady-state regime. **d)** Histogram superposition for umbrella sampling simulations. A set of 17 windows was used to recover free energy profiles.

Stalk formation in the presence of one C2B wild-type domain and one C2B T328E,T329E mutant domain

To support the evidence for the proposed master-servant mechanism, we have conducted PMF calculations using a combination of wild-type and mutant C2B domains. Again, for adequate comparison, the rest of the system and the collective variable parameters were kept identical to the rest of the simulations along this work. Figure S16a shows the free energy profile for the C2B-WT-Mut system (red line), compared to the rest of the systems. It can be observed that in free energy terms for fusion stalk formation, the combination of a wild-type and a mutant T328E,T329E domain has similar effects than the system containing two wild-type domains (red line is only slightly above the blue one). This result verifies that even with one mutated C2B domain, the master-servant cooperation is still robust. As shown before, to significantly reduce the cooperation (making the free energy to rise above the membranes-only curve) two mutant domains are needed.

Additionally, we have conducted 5μs of unbiased simulations initiated from flat and parallel bilayers containing the two C2B domains (one wild-type and one T328E,T329E mutant) in the inter-membrane space (the cytosol). Figure S16b shows the inter-membrane distance for this system together with the rest of the systems showed in figure 5b in the main text. It can be observed that wild-type and mutant domains (red line) pull membranes together more effectively than than the system with 2 Syt1-C2B mutant (green line) domains but significantly less effectively than the system with 2 Syt1-C2B wild-type domains (blue line). Again, in agreement with the free energy profile in S16a this result verifies the intermediate situation between 2 C2B wild-type domains and 2 C2B mutant domains.

Panels S16c and S16d show convergence analysis for the wild-type and mutant T328E,T329E system.

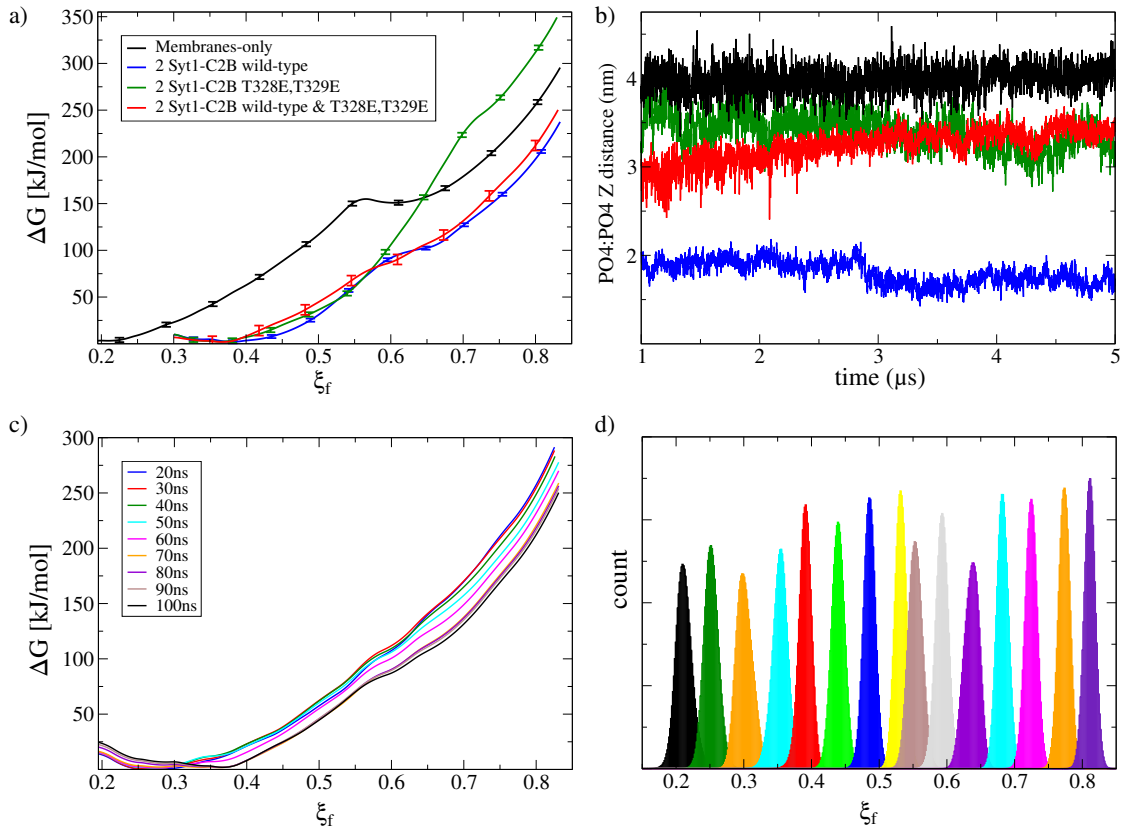

Figure S16: **Wild-type and mutant T328E,T329E C2B domains**. **a)** PMF for fusion stalk formation. **b)** PO4:PO4 inter-membrane distance. **c)** Free energy profiles at different simulation times in the steady-state regime. **d)** Histogram superposition for umbrella sampling simulations. A set of 15 windows was used to recover free energy profiles.

PLUMED: input file to induce a stalk at $\xi_f \sim 0.85$

```
INCLUDE FILE=groups.dat

memFusion: MEMFUSION UMEMBRANE=uMem LMEMBRANE=lMem TAILS=tails NSMEM=85 DSMEM=0.1

HMEM=0.25 RCYLMEM=1.75 ZETAMEM=0.5

MOVINGRESTRAINT ...

ARG=memFusion

STEP0=0 AT0=0.3 KAPPA0=10000.0

STEP1=500000 AT1=1.0 KAPPA1=10000.0

...

PRINT ARG=memFusion FILE=COLVAR STRIDE=1
```

PLUMED: groups.dat

```
lMem: GROUP ATOMS=1-10752,21505-22728,23953-24420

uMem: GROUP ATOMS=10753-21504,22729-23952,24421-24888

tails: GROUP ATOMS=8-23948:12,12-23952:12,23966-24884:18,23970-24888:18
```